IDE**▲**L®

Cross-Correlated Quadrupolar Spin Relaxation and Carbon-13 Lineshapes in the $^{13}CD_2$ Spin Grouping

L. G. Werbelow,* G. A. Morris,† P. Kumar,‡ and J. Kowalewski‡

*Chemistry Department, NMIMT, Socorro, New Mexico 87801; †Department of Chemistry, University of Manchester, Oxford Road, Manchester M13 9PL, United Kingdom; and ‡Physical Chemistry, Arrhenius Laboratory, Stockholm University, S-106 91 Stockholm, Sweden

Lineshape calculations are reported for a spin system consisting of a spin-$\frac{1}{2}$ nucleus scalar-coupled to two magnetically equivalent spin-1 nuclei, e.g., a CD_2 group. It is found that, because of the differential line broadening, the peak height ratio of the five spin-$\frac{1}{2}$ nucleus transitions is expected to deviate from the integrated intensity ratio of 1:2:3:2:1. The deviation is dependent on the extent of cross-correlation between the two quadrupolar interactions. The theoretical predictions for peak height ratios and for bandshapes are tested for the carbon-13 spectrum of perdeuterated ethylene glycol, and iterative fitting is used to obtain an estimate of the extent of the correlation between the quadrupolar interactions for the two deuterons. © 1999 Academic Press

Key Words: cross-correlation; quadrupolar relaxation; carbon-13 multiplet; reference deconvolution.

INTRODUCTION

Cross-correlation or interference effects in nuclear magnetic spin relaxation studies provide simple access to abundant microdynamical information (*1*). One of the more fascinating possibilities of utilising interference effects relates to unique "T_1" interferences revealed through lineshape investigations of less efficiently relaxed, coupled spins (*2–4*).

In the present study, the appropriate lineshape calculation for an isolated $A(I = \frac{1}{2})X_2(S = 1)$ (e.g., $^{13}CD_2$) spin grouping is examined. It is demonstrated that it is possible to measure quadrupole–quadrupole cross-correlation indirectly through the lineshapes of spin-$\frac{1}{2}$ nuclei, for which transverse relaxation is relatively inefficient and easily dominated by quadrupolar relaxation pathways associated with higher-order spin. At present, the only access to such correlation has been through multiquantum studies (*5*) or investigations of spins embedded in spatially anisotropic environments (*6*).

THEORY

In the subsequent development, it is assumed that the two deuterons (spins S and S') are magnetically equivalent and relaxed efficiently by axially symmetric quadrupolar interac-

tions. It is initially assumed that all members of the ^{13}C (spin I) pentet are well resolved, extreme narrowing obtains, and all ^{13}C line broadening results from deuteron T_1 processes; the latter requirement is then removed. Any or all of the remaining assumptions can be removed quite simply, but for the points we wish to illustrate, such generalizations are unnecessary.

The appropriate basis states that diagonalize $\mathcal{H}_0 = -(\omega_I - \mathcal{J}_{IS}S_z)I_z - \omega_S(S_z + S'_z) + \mathcal{J}_{SS'}S \cdot S'$ are labeled as follows: $|i\rangle = |m_I m_S m_{S'}\rangle$, where $m_I = \alpha(+\frac{1}{2})$, $\beta(+\frac{1}{2})$ and $m_S(m_{S'}) = 1, 0, -1$:

$$|1\rangle = |\alpha11\rangle,$$

$$|2\rangle = (|\alpha10\rangle + |\alpha01\rangle)/\sqrt{2},$$

$$|3\rangle = (|\alpha10\rangle - |\alpha01\rangle)/\sqrt{2},$$

$$|4\rangle = (|\alpha1-1\rangle + |\alpha-11\rangle + 2|\alpha00\rangle)/\sqrt{6},$$

$$|5\rangle = (|\alpha1-1\rangle - |\alpha-11\rangle)/\sqrt{2},$$

$$|6\rangle = (|\alpha1-1\rangle + |\alpha-11\rangle - |\alpha00\rangle)/\sqrt{3},$$

$$|7\rangle = (|\alpha-10\rangle - |\alpha0-1\rangle)/\sqrt{2},$$

$$|8\rangle = (|\alpha-10\rangle + |\alpha-01\rangle)/\sqrt{2},$$

$$|9\rangle = |\alpha-1-1\rangle,$$

$$|10\rangle = |\beta11\rangle,$$

$$|11\rangle = (|\beta10\rangle + |\beta01\rangle)/\sqrt{2},$$

$$|12\rangle = (|\beta10\rangle - |\beta01\rangle)/\sqrt{2},$$

$$|13\rangle = (|\beta1-1\rangle + |\beta-11\rangle + 2|\beta00\rangle)/\sqrt{6},$$

$$|14\rangle = (|\beta1-1\rangle - |\beta-11\rangle)/\sqrt{2},$$

$$|15\rangle = (|\beta1-1\rangle + |\beta-11\rangle - |\beta00\rangle)/\sqrt{3},$$

$$|16\rangle = (|\beta-10\rangle - |\beta0-1\rangle)/\sqrt{2},$$

$$|17\rangle = (|\beta-10\rangle + |\beta-01\rangle)/\sqrt{2},$$

$$|18\rangle = |\beta-1-1\rangle.$$

Ⓐ🅟

Notation can be simplified by contracting each pair of indices for a coherence χ into one: $\chi_{i,i+9} \Rightarrow \chi_i$.

Application of standard theory (7–9) demonstrates that the free evolution of ^{13}C single quantum coherence for a CD_2 group is described by the partially coupled expressions

$$-(d/dt)\chi_1 = [i\{\omega_C - 4\pi J_{CD}\} + 24J]\chi_1, \qquad [1]$$

$$-(d/dt)\begin{bmatrix} \chi_2 \\ \chi_3 \end{bmatrix} = \left(i\{\omega_C - 2\pi J_{CD}\}\begin{bmatrix} 1 & 0 \\ 0 & 1 \end{bmatrix} \right.$$
$$\left. + \begin{bmatrix} 26J + 2K & -6J + 6K \\ -6J + 6K & 26J - 14K \end{bmatrix} \right)\begin{bmatrix} \chi_2 \\ \chi_3 \end{bmatrix},$$
$$[2]$$

$$-(d/dt)\begin{bmatrix} \chi_4 \\ \chi_5 \\ \chi_6 \end{bmatrix}$$

$$= \begin{bmatrix} i\omega_C + 24J & 0 & -\dfrac{16}{3}(J+K) \\ 0 & i\omega_C + 24J - 16K & 0 \\ -\dfrac{16}{3}(J+K) & 0 & i\omega_C + \dfrac{80}{3}(J+K) \end{bmatrix}$$

$$\times \begin{bmatrix} \chi_4 \\ \chi_5 \\ \chi_6 \end{bmatrix}, \qquad [3]$$

$$-(d/dt)\begin{bmatrix} \chi_7 \\ \chi_8 \end{bmatrix} = \left(i\{\omega_C + 2\pi J_{CD}\}\begin{bmatrix} 1 & 0 \\ 0 & 1 \end{bmatrix} \right.$$
$$\left. + \begin{bmatrix} 26J - 14K & -6J + 6K \\ -6J + 6K & 26J + 2K \end{bmatrix} \right)\begin{bmatrix} \chi_7 \\ \chi_8 \end{bmatrix},$$
$$[4]$$

$$-(d/dt)\chi_9 = [i\{\omega_C + 4\pi J_{CD}\} + 24J]\chi_9, \qquad [5]$$

where J and K are the autocorrelation and cross-correlation quadrupolar spectral densities, respectively, ω_C is the offset from resonance of the carbon-13 chemical shift, and J_{CD} is the carbon–deuterium one-bond coupling constant. The presumption of well-resolved lines (the secular approximation) effectively zeros all other couplings. However, Eqs. [1]–[5] do assume that the two deuterons are magnetically equivalent. If temporal fluctuations distinguish between these two spins, then the size of $J(K)$ compared with the very small deuteron–deuteron spin–spin coupling is relevant and the description becomes considerably more complicated.

For axially symmetric molecular diffusion (characterized by the rotational diffusion coefficients $D_\perp$, $D_\parallel$), the autocorrelation and cross-correlation quadrupolar spectral densities are defined as (7)

$$J = (3/640)(e^2qQ/\hbar)^2[(3\cos^2\theta - 1)^2\tau_{20}$$
$$+ 12(\sin^2\theta \cos^2\theta)\tau_{21} + 3\sin^4\theta\tau_{22}], \qquad [6]$$

$$K = (3/640)(e^2qQ/\hbar)^2[(3\cos^2\theta - 1)^2\tau_{20}$$
$$+ 12(\sin^2\theta \cos^2\theta)\cos(\phi - \phi')\tau_{21}$$
$$+ 3\sin^4\theta \cos(2\phi - 2\phi')\tau_{22}], \qquad [7]$$

where eQ is the nuclear quadrupole moment, eq is the field gradient, $1/\tau_{2n} = 6D_\perp + n^2(D_\parallel - D_\perp)$, θ is the angle between the principal axis of the quadrupole interaction and the principal axis of the diffusion tensor, and $\phi - \phi'$ is the angle, when viewed along the principal diffusion axis, between the two quadrupole axes.

Although the integrated intensities of the ^{13}C pentet are in the ratio of 1:2:3:2:1, the apparent heights of the multiplet components do not obey this simple pattern because of differential line broadening. This behavior is similar to the situation for the ^{13}C triplet associated with the ^{13}C–^2H grouping, where the apparent simple Lorentzian heights, in the same limit, are in the ratio 2:3:2 (10). As might be expected, quadrupolar broadened lines in the CD_2 grouping are somewhat broader than the corresponding lines in the CD grouping. For example, assuming similar correlation times and quadrupolar coupling constants, the outermost ^{13}C multiplet components are twice as broad in $^{13}CD_2$, $\frac{6}{5}(1/T_{1Q})$, as in ^{13}CD, $\frac{3}{5}(1/T_{1Q})$. $1/T_{1Q}$ denotes the quadrupolar spin–lattice relaxation rate of the deuteron, equal in the extreme narrowing regime to $20J$ (11), and the linewidths are given as half-widths at half-height in rad per second.

More interestingly, whenever the ^{13}C resonances are homogeneously broadened by deuteron quadrupolar interactions, the apparent heights of the five lines depend on the degree of correlation between the two quadrupolar interactions. To calculate the apparent peak heights, it is important to recognize that the outermost lines are described by a single Lorentzian (Eqs. [1] and [5]), whereas the inner lines (cf. Eqs. [2] and [4]) and the central peak (Eq. [3]) consist of two and three Lorentzian components, respectively. Despite this relative complexity, the bandshape

$$I(\omega) \propto \text{Re} \int \langle \mathbf{I}_+(t)\mathbf{I}_-(0)\rangle \exp(-i\omega t)dt \qquad [8]$$

can be solved analytically and written in the form

$$I(\omega) \propto \frac{24J}{(24J)^2 + (\omega_C - 4\pi J_{CD} - \omega)^2}$$

$$+ \frac{16(64J - 24K)(40J^2 - 15JK - 4K^2) + 40J(\omega_C - 2\pi J_{CD} - \omega)^2}{(16(40J^2 - 15JK - 4K^2))^2 + 16(89J^2 - 48JK + 17K^2)(\omega_C - 2\pi J_{CD} - \omega)^2 + (\omega_C - 2\pi J_{CD} - \omega)^4}$$

$$+ \frac{\frac{2}{3}(92J + 56K)\left(-\frac{256}{9}(J + K)^2 + (24J)\left(\frac{80}{3}(J + K)\right)\right) + (40J + 16K)(\omega_C - \omega)^2}{\left(-\frac{256}{9}(J + K)^2 + (24J)\left(\frac{80}{3}(J + K)\right)\right)^2 + \left(\left(\frac{512}{9}(J + K)^2 + (24J)^2 + \left(\frac{80}{3}(J + K)\right)^2\right)(\omega_C - \omega)^2 + (\omega_C - \omega)^4}$$

$$+ \frac{24J - 16K}{(24J - 16K)^2 + (\omega_C - \omega)^2}$$

$$+ \frac{16(64J - 24K)(40J^2 - 15JK - 4K^2) + 40J(\omega_C + 2\pi J_{CD} - \omega)^2}{(16(40J^2 - 15JK - 4K^2))^2 + 16(89J^2 - 48JK + 17K^2)(\omega_C + 2\pi J_{CD} - \omega)^2 + (\omega_C + 2\pi J_{CD} - \omega)^4}$$

$$+ \frac{24J}{(24J)^2 + (\omega_C + 4\pi J_{CD} - \omega)^2}. \tag{9}$$

Thus, it follows that in the absence of extraneous line broadening the apparent peak heights of the five components are in the ratios

$$1 : \frac{12(8 - 3\xi)}{(40 - 15\xi - 4\xi^2)} : \frac{3(293 + 70\xi - 88\xi^2)}{(258 + 74\xi - 176\xi^2 + 8\xi^3)} :$$

$$\frac{12(8 - 3\xi)}{(40 - 15\xi - 4\xi^2)} : 1, \tag{10}$$

where the correlation factor, ξ, is defined as K/J.

$$-(d/dt)\chi_1 = [i\{\omega_C - 4\pi J_{CD}\} + 24J + r]\chi_1, \tag{11}$$

$$-(d/dt)\begin{bmatrix} \chi_2 \\ \chi_3 \end{bmatrix}$$

$$= \left(i\{\omega_C - 2\pi J_{CD}\}\begin{bmatrix} 1 & 0 \\ 0 & 1 \end{bmatrix} \right.$$

$$\left. + \begin{bmatrix} 26J + 2K + r & -6J + 6K \\ -6J + 6K & 26J - 14K + r \end{bmatrix} \right)\begin{bmatrix} \chi_2 \\ \chi_3 \end{bmatrix}, \tag{12}$$

$$-(d/dt)\begin{bmatrix} \chi_4 \\ \chi_5 \\ \chi_6 \end{bmatrix} = \begin{bmatrix} i\omega_C + 24J + r & 0 & -\frac{16}{3}(J + K) \\ 0 & i\omega_C + 24J - 16K + r & 0 \\ -\frac{16}{3}(J + K) & 0 & i\omega_C + \frac{80}{3}(J + K) + r \end{bmatrix}\begin{bmatrix} \chi_4 \\ \chi_5 \\ \chi_6 \end{bmatrix}, \tag{13}$$

So far it has been assumed that the carbon-13 transverse relaxation is dominated by the one-bond scalar coupling to deuterium. In practice this will frequently not be the case, since both instrumental effects, such as field inhomogeneity, and other sources of transverse relaxation will contribute to the carbon-13 linewidths. This broadening will reduce the deviations of the peak height ratios from 1:2:3:2:1. The effects of these extraneous sources of line broadening can be included in the analysis above by adding terms in the extraneous decay rate r to Eqs. [1] to [5] above, where the extra line broadening corresponds to r/π Hz full width at half-height:

$$-(d/dt)\begin{bmatrix} \chi_7 \\ \chi_8 \end{bmatrix}$$

$$= \left(i\{\omega_C + 2\pi J_{CD}\}\begin{bmatrix} 1 & 0 \\ 0 & 1 \end{bmatrix} \right.$$

$$\left. + \begin{bmatrix} 26J - 14K + r & -6J + 6K \\ -6J + 6K & 26J + 2K + r \end{bmatrix} \right)\begin{bmatrix} \chi_7 \\ \chi_8 \end{bmatrix}, \tag{14}$$

$$-(d/dt)\chi_9 = [i\{\omega_C + 4\pi J_{CD}\} + 24J + r]\chi_9. \tag{15}$$

The analytical solution for the total lineshape, given in Table 1,

$$
I(\omega) \propto \frac{24J + r}{(24J + r)^2 + (\omega_C - 4\pi J_{CD} - \omega)^2}
$$

$$
+ \frac{(64J - 24K + 2r)(640J^2 - 240JK - 64K^2 + 52Jr - 12Kr + r^2) + (40J + 2r)(\omega_C - 2\pi J_{CD} - \omega)^2}{(-36(J - K)^2 + (26J - 14K + r)(26J + 2K + r))^2 + (72(J - K)^2 + (26J - 14K + r)^2 + (26J + 2K + r)^2)(\omega_C - 2\pi J_{CD} - \omega)^2 + (\omega_C - 2\pi J_{CD} - \omega)^4}
$$

$$
+ \frac{24J - 16K + r}{(24J - 16K + r)^2 + (\omega_C - \omega)^2}
$$

$$
+ \frac{\frac{2}{3}(92J + 56K + 3r)\left(-\frac{256}{9}(J + K)^2 + (24J + r)\left(\frac{80}{3}(J + K) + r\right)\right) + 2(20J + 8K + r)(\omega_C - \omega)^2}{\left(-\frac{256}{9}(J + K)^2 + (24J + r)\left(\frac{80}{3}(J + K) + r\right)\right)^2 + \left(\left(\frac{512}{9}(J + K)^2 + (24J + r)^2 + \left(\frac{80}{3}(J + K) + r\right)^2\right)(\omega_C - \omega)^2 + (\omega_C - \omega)^4\right)}
$$

$$
+ \frac{(64J - 24K + 2r)(640J^2 - 240JK - 64K^2 + 52Jr - 12Kr + r^2) + (40J + 2r)(\omega_C + 2\pi J_{CD} - \omega)^2}{(-36(J - K)^2 + (26J - 14K + r)(26J + 2K + r))^2 + (72(J - K)^2 + (26J - 14K + r)^2 + (26J + 2K + r)^2)(\omega_C + 2\pi J_{CD} - \omega)^2 + (\omega_C + 2\pi J_{CD} - \omega)^4}
$$

$$
+ \frac{24J + r}{(24J + r)^2 + (\omega_C + 4\pi J_{CD} - \omega)^2}
$$

is similar in form to Eq. [9]. The expressions for the peak height ratios become

$$
1 : \frac{2(24 + \rho)(32 - 12\xi + \rho)}{(640 - 64\xi^2 + 52\rho + \rho^2 - 12\xi(20 + \rho))} \quad [16]
$$

for the ratio of the peak height of the inner lines (at $\pm J_{CD}$) to that of the outer lines, and

$$
1 : \frac{(24 + \rho)}{(24 - 16\xi + \rho)}
$$

$$
+ \frac{6(92 + 56\xi + 3\rho)(24 + \rho)}{(5504 - 256\xi^2 + 456\rho + 9\rho^2 + 16\xi(328 + 15\rho))} \quad [17]
$$

for the ratio of the central line to the outer lines, where ρ is the extraneous transverse decay rate r divided by the autocorrelation spectral density J.
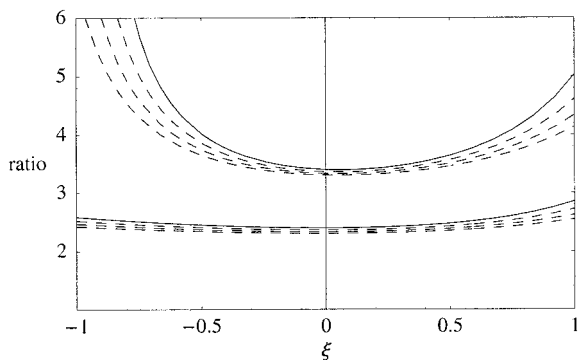

FIG. 1. Predicted relative peak heights of inner and central lines in a carbon-13 pentet from a CD$_2$ group with respect to the outer lines, as a function of the ratio ξ of the quadrupolar cross- and autocorrelation spectral density functions, for extraneous decay rates (solid line) $\rho = 0$ and (dashed lines, top to bottom) $\rho = 2T$, $4T$, and $6T$.
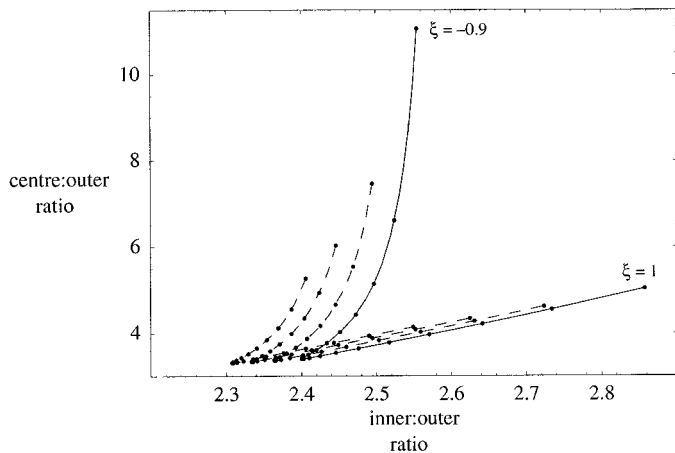

FIG. 2. Loci of the peak height ratios inner:outer and central:outer for a CD$_2$ group as the cross-correlation factor ξ varies from 1.0 to -0.9 in steps of 0.1 (solid circles), for extraneous decay rates (solid line) $\rho = 0$ and (dashed lines, right to left) $\rho = 2T$, $4T$, and $6T$.
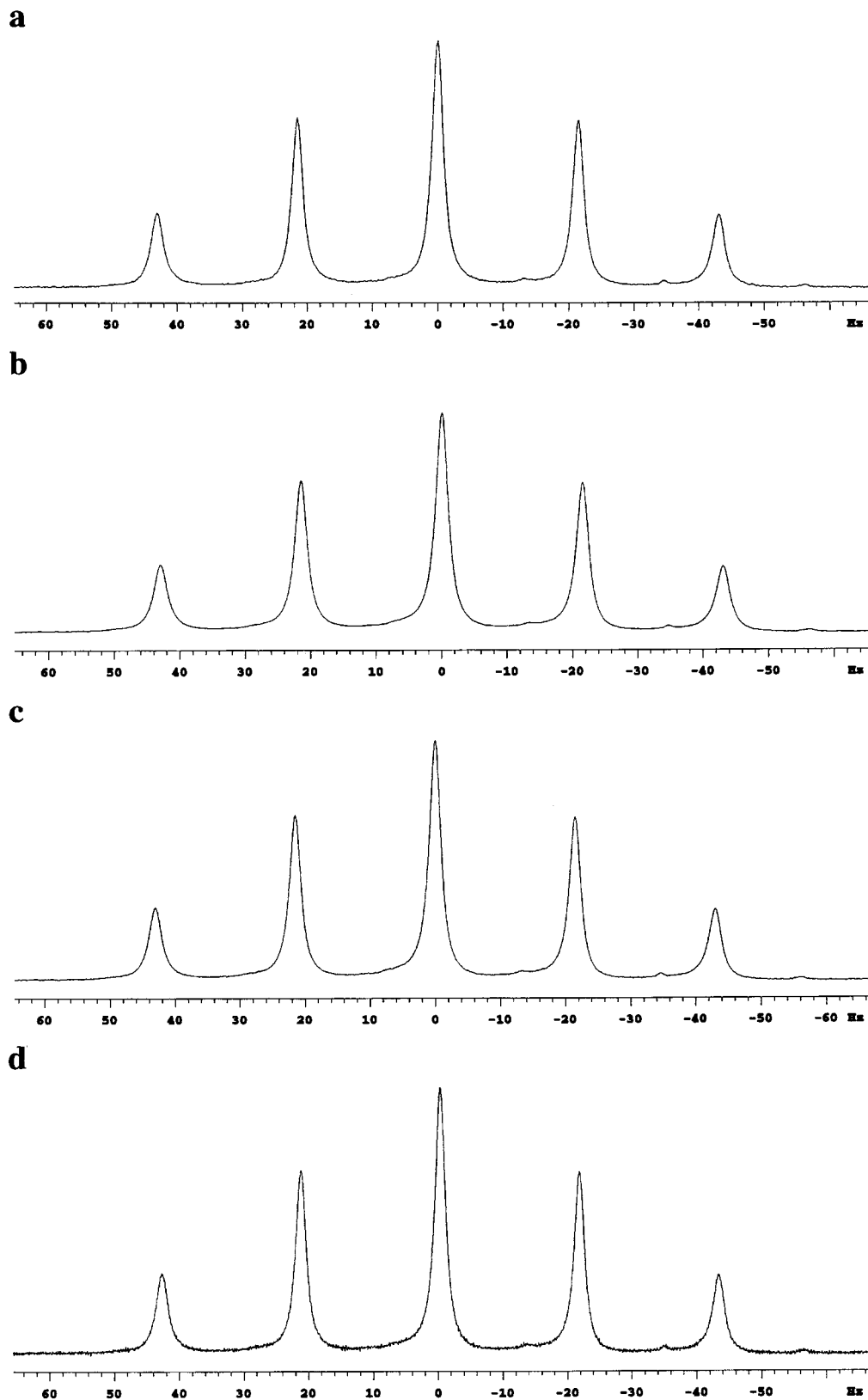
FIG. 3. Carbon-13 spectra of the CD_2 group in perdeuterated ethylene glycol at 323 K: (a) spectrum obtained by Fourier transformation of the original FID, without any artificial line broadening; (b) spectrum obtained by reference deconvolution using one of the lines of the acetonitrile methyl signal as the lineshape reference, with a target lineshape of a Lorentzian of full width at half-height 0.3 Hz; (c) spectrum obtained by reference deconvolution with a 0.2-Hz target linewidth; (d) spectrum obtained by reference deconvolution with a target linewidth of 0.1 Hz.

TABLE 2
Experimental Relative Peak Heights of the Central Line and (Averaged) Inner Line with Respect to (Averaged) Outer Line for the CD$_2$ Group in Perdeuterated Ethylene Glycol[a]

T (K)	T_{1Q} (s)	T_1 (s)		LB (Hz)	Inner	Central
		Glycol	Methyl			
323	0.23	27	15.7	0.3	2.31	3.40
				0.2	2.34	3.43
				0.1	2.40	3.55
333	0.31	30	16.0	0.3	2.43	3.40
				0.2	2.34	3.35
				0.1	2.43	3.57
343	0.40	40	16.0	0.3	2.32	3.38
				0.2	2.34	3.22
				0.1	2.36	3.43

[a] The data were obtained using FIDDLE (*13*) with different values of line broadening (LB).

The peak height ratios as a function of the correlation factor ξ for different values of the extraneous linewidth parameter ρ are shown in Fig. 1. As expected, the sensitivity of the ratios to the value of ξ decreases as ρ increases. The flat, almost symmetric region of Fig. 1 close to $\xi = 0$ shows that the peak height ratios are relatively poor indicators of the sign and magnitude of small values of ξ. It is, however, not immediately obvious from Fig. 1 how readily a value of ξ may be deduced for other peak height ratios. Figure 2 shows the locus of the peak height ratios as a function of ξ for a series of values of ρ. As expected, close to $\xi = 0$ the locus varies only slowly with ξ, but for larger magnitudes the peak height ratios form an unambiguous indicator of both sign and magnitude of ξ. The effect of the extraneous broadening ρ is, as expected, to reduce the sensitivity of the peak height ratio to ξ, but interestingly the peak height ratios define unique values of both ξ and ρ for most combinations of ratios. The peak height ratios are most characteristic for more negative values of ξ. If the peak height ratios can be determined accurately, then only at the intersections of the loci of Fig. 2 is there any ambiguity. As will be seen, however, the accuracy requirements for the peak height ratios may be difficult to meet in practice, and a method that

makes fuller use of the experimental data may be more appropriate.

RESULTS AND DISCUSSION

To investigate experimentally the deviations from the 1:2:3:2:1 peak height ratio for a CD$_2$ pentet, one should select a system for which the deuteron T_{1Q} is in a suitable range. The quadrupolar relaxation rate should be small enough not to cause the collapse of the pentet and yet large enough to cause a distinct broadening of the carbon lines. By analogy with the $A(I = \frac{1}{2})X(S = 1)$ spin system discussed by Pople (*10*), the condition can be specified as

$$\frac{r}{\pi} < \frac{1}{\pi T_{1Q}} < J_{CD}, \qquad [18]$$

where r is the extraneous transverse relaxation rate of the carbon spin due to other mechanisms, introduced above, and T_{1Q} is the deuteron spin–lattice relaxation time. With a typical CD scalar coupling constant of 20–25 Hz, we can expect a T_{1Q} of a few hundred milliseconds to be suitable. This corresponds to a rotational correlation time (assumed isotropic) of the order of 10 ps for a deuteron quadrupolar coupling constant of about 170 kHz. These desired magnitudes of the correlation time and quadrupolar relaxation time can be realized in neat perdeuterated ethylene glycol above room temperature. Although ethylene glycol shows a two-bond coupling between carbon-13 and deuterium, the small magnitude of the coupling constant (-0.3 Hz) and the relatively rapid deuterium spin–lattice relaxation mean that the contribution to scalar relaxation from this source should be relatively small.

With these considerations in mind, we have measured carbon-13 spectra of a sample containing 95% (by volume) perdeuterated ethylene glycol and 5% carbon-13-enriched acetonitrile. Carbon-13 spectra were taken at 323, 333, and 343 K, using a Varian Inova 400 NMR spectrometer, operating at 9.4 T. A 5-mm-o.d. sample tube was used in a modified Jeol C/H 5-mm probe. The temperature was controlled using the standard Varian VT controller. The spectra were obtained with a spectral width of 14,000 Hz, using 330K data points and a 90°

TABLE 3
Results of Fitting the Analytical Formula of Table 1 to the Three Experimental Spectra of Perdeuterated Ethylene Glycol after Deconvolution with a 0.2-Hz-Wide Lorentzian Target Lineshape[a]

T (K)	J (fixed) (s^{-1})	K (s^{-1})	ξ	r (s^{-1})	J_{CD} (Hz)
323	0.217	0.084 ± 0.020	0.39 ± 0.09	1.64 ± 0.06	21.52 ± 0.01
333	0.161	0.045 ± 0.028	0.28 ± 0.18	1.48 ± 0.06	21.54 ± 0.01
343	0.125	0.032 ± 0.034	0.26 ± 0.26	1.23 ± 0.07	21.55 ± 0.01

[a] Errors quoted are ± 2 estimated standard errors.

a

−60   −40   −20   0 Hz   20   40   60

b

−60   −40   −20   0 Hz   20   40   60

c

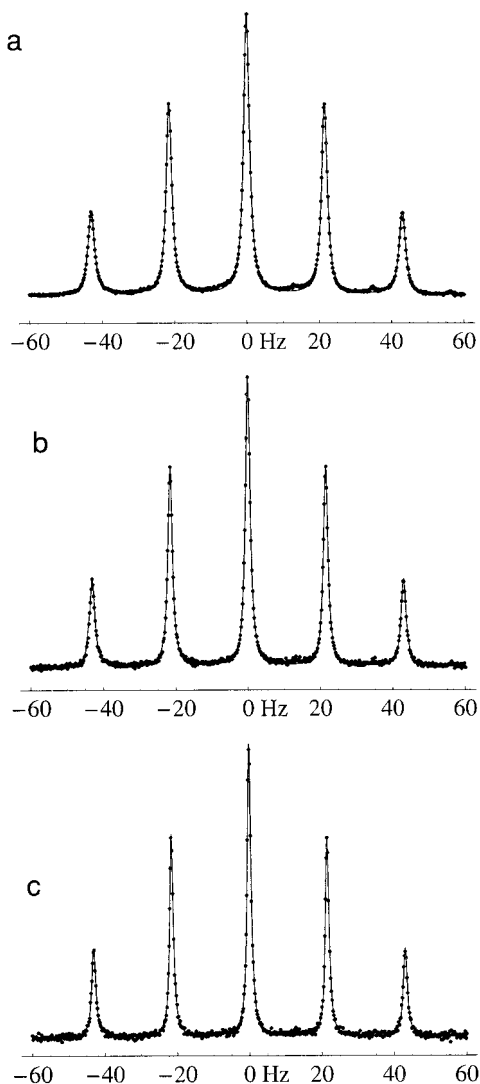−60   −40   −20   0 Hz   20   40   60

FIG. 4. Experimental (solid circles) and simulated (solid lines) spectra for the CD_2 group in perdeuterated ethylene glycol at (a) 323 K, (b) 333 K, and (c) 343 K.

pulse duration of 13.5 μs. A recycle delay of 170 s was used, with 256 transients. Since every experiment took about 12 h, field/frequency stabilization by means of deuterium lock was essential. As expected given the very low average deuterium radiofrequency field strength of the field/frequency lock channel, the application of the deuterium signal for the field/frequency locking had no effect on the measured lineshape of the carbon pentet in a short test experiment. The carbon-13 and deuteron spin–lattice relaxation times were measured using the fast inversion–recovery technique (12). Deuteron measurements were performed, without field/frequency lock, on the same sample using a Varian 10-mm broadband probe; the 90° pulse duration for this probe was 35 μs.

The reason for adding carbon-13-enriched acetonitrile to the

glycol sample was that we wanted to have a reference signal characterizing the inhomogeneous lineshape. The inhomogeneous broadening was about 0.3–0.4 Hz, which is not negligible compared with the natural linewidth. To reduce the influence of the B_0 inhomogeneity on the measured peak heights, and to remove any bias caused by the distinctly non-Lorentzian character of the instrumental lineshape, we performed reference deconvolution using the program FIDDLE (13). The lineshapes of the acetonitrile methyl signal were successively replaced by Lorentzians of width 0.3, 0.2, and 0.1 Hz for each of the three experimental spectra using FIDDLE; Fig. 3 shows the resultant spectra for 323 K. This process effectively replaces the instrumental lineshape by a Lorentzian of width equal to the width specified less the natural linewidth of the reference signal, which in the case of acetonitrile should be a few hundredths of a hertz. The peak height ratios for the CD_2 pentet, determined by eye to minimize the effects of noise, are summarized in Table 2. The table also contains the deuteron spin–lattice relaxation time T_{1Q} as well as the experimentally determined T_1 for carbon-13 of the perdeuterated glycol and for the methyl group in acetonitrile. The carbon T_1 values place an upper limit on the time constant $1/r$ for extraneous spin–spin relaxation of the glycol carbon-13, while the deuteron T_{1Q} values give an independent measure of the autocorrelation spectral density J.

We can see from the data of Table 2 that the perdeuterated glycol sample used does indeed fulfil the inequality [18]. We see also that the experimental peak height ratios deviate significantly from 1:2:3:2:1 integrated intensity ratio, and that the deviations are most significant when the inhomogeneous broadening is minimized (deconvolution target lineshape of a 0.1-Hz Lorentzian). Locating the peak height ratios on Fig. 2, several interesting points emerge. Firstly, the ratios are relatively low, lying toward the bottom left-hand corner of Fig. 2, showing that the extraneous line broadening is significant compared with the autocorrelation spectral density, even when the instrumental broadening is reduced to only 0.1 Hz. Second, the peak height ratios cluster, unfortunately, in the region corresponding to small magnitudes of ξ. Finally, and equally disappointingly, the experimental uncertainties in peak height ratio evident from the scatter in the values in Table 2, and to be expected from the limits of signal-to-noise ratio in the experimental spectra, prevent accurate determination of ξ and ρ from the peak height data.

The peak heights, however, represent only a small fraction of the data available. The complete bandshape contains information on the widths as well as the relative amplitudes of the nine individual Lorentzian components of the five lines, and hence characterizes the coherence dynamics much more fully than the peak height ratios, in addition to providing statistically more reliable data. To allow full iterative fitting of the experimental bandshape, the spectral data for the CD_2 region at 323, 333, and 343 K were deconvoluted to a target lineshape of a 0.2-Hz Lorentzian, baseline corrected, and transferred to a PowerMacin-

tosh 7600/132 computer running Mathematica 3.0 (*14*). Nonlinear fitting software based on the Levenberg–Marquardt algorithm was used to fit the analytical formula of Table 1 to the three sets of experimental data, allowing the signal intensities, cross-correlation spectral densities K, coupling constants J_{CD}, extraneous decay rates r, and offsets from resonance to vary, but with the autocorrelation spectral densities J fixed at the values calculated from the deuteron spin–lattice relaxation times listed in Table 2. The results, listed in Table 3, show that although the standard errors on the cross-correlation spectral densities K obtained from the three fits are relatively large, the data are still sufficient to identify the sign of ξ as positive, and all three fits are consistent with approximately 35% cross-correlation. The extraneous decay rates r correspond to full linewidths at half-height of 0.4–0.5 Hz, significantly greater than the known instrumental broadening after deconvolution of just under 0.2 Hz. The extra broadening is roughly consistent with the order of magnitude expected for scalar relaxation of the second kind via the two-bond carbon–deuterium coupling, but decreases slightly with temperature instead of increasing; it is possible that there is also a contribution from chemical exchange. Figure 4 shows the fit between simulation and experiment for the three deconvoluted experimental spectra; the broadening of the small impurity signals to high field with increasing temperature also suggests the presence of an exchange process.

In conclusion, we have predicted and demonstrated the occurrence of differential line broadening in the carbon pentet of a CD_2 group. We have shown that it is in principle possible to estimate the extent of correlation between the quadrupolar interactions for the two deuterons using the peak height ratios in the pentet, and that a more accurate measure can be obtained by direct iterative fitting of the experimental bandshape.

ACKNOWLEDGMENTS

REFERENCES

1. D. M. Grant and R. A. Brown, *in* "Encyclopedia of Nuclear Magnetic Resonance" (D. M. Grant and R. K. Harris, Eds.), p. 4003, Wiley, Chichester, (1996); M. M. Fuson, *in* "Encyclopedia of Nuclear Magnetic Resonance" (D. M. Grant and R. K. Harris, Eds.), p. 1466, Wiley, Chichester (1996); C. L. Mayne and S. A. Smith, *in* "Encyclopedia of Nuclear Magnetic Resonance" (D. M. Grant and R. K. Harris, Eds.), p. 4053, Wiley, Chichester (1996); T. C. Farrar and T. C. Stringfellow, *in* "Encyclopedia of Nuclear Magnetic Resonance" (D. M. Grant and R. K. Harris, Eds.), p. 4101. Wiley, Chichester (1996).

2. L. G. Werbelow, A. Allouche, and G. Pouzard, *J. Chem. Soc. Faraday Trans. 2* **83**, 871 (1987).

3. L. G. Werbelow, *J. Magn. Reson.* **67**, 66 (1986).

4. L. G. Werbelow and R. E. London, *J. Chem. Phys.* **102**, 5181 (1995).

5. A. Wokaun and R. R. Ernst, *Mol. Phys.* **36**, 317 (1978).

6. R. Poupko, R. L. Vold, and R. R. Vold, *J. Magn. Reson.* **34**, 67 (1979).

7. L. G. Werbelow, *in* "Nuclear Magnetic Probes of Molecular Dynamics" (R. Tycko, Ed.), Plenum, New York, 1994.

8. A. G. Redfield, *Adv. Magn. Reson.* **1**, 1 (1966); P. S. Hubbard, *Rev. Mod. Phys.* **33**, 249 (1961).

9. A. Abragam, "Principles of Nuclear Magnetic Resonance," p. 448ff, Oxford (1970).

10. J. A. Pople, *Mol. Phys.* **1**, 168 (1958).

11. L. G. Werbelow, *in* "Encyclopedia of Nuclear Magnetic Resonance" (D. M. Grant and R. K. Harris, Eds.), p. 4092, Wiley, Chichester (1996).

12. D. Canet, G. C. Levy, and I. R. Peat, *J. Magn. Reson.* **18**, 199 (1975).

13. G. A. Morris, H. Barjat, and T. J. Horne, *Progr. NMR Spectrosc.* **31**, 197 (1997).

14. S. Wolfram, "The Mathematica Book," 3rd ed., Wolfram Media/Cambridge Univ. Press, Cambridge (1996).